

Heavy Flavor Tracker (HFT) : a new inner tracking device at STAR

Jonathan Bouchet¹, for the STAR collaboration

¹ Kent State University, Ohio, USA



Abstract

Due to their large masses, heavy flavor (c and b quarks) are produced in the early stages of heavy ion collision [1]. The measurement of charm meson nuclear modification factor R_{AA} , as well as their flow velocity will be investigated by the HFT. A precise measurement of heavy flavor production could be achieved by identifying the decay of charm meson using direct topological reconstruction and thus disentangling the b and c quarks. The HFT is a proposed new inner tracking detector for STAR.

Introduction : the physics of HFT

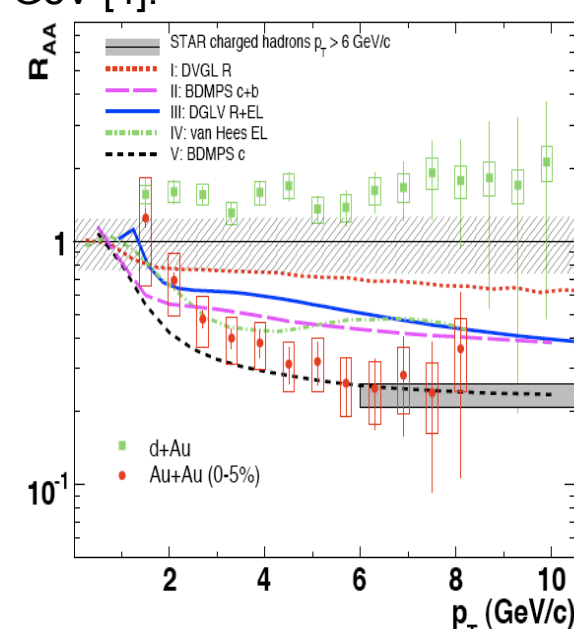
The studies of high energies collisions occurred RHIC are supposed to give insights about the nuclear matter at extreme temperatures and energy densities and describe the so-called Quark-Gluon Plasma. Investigation of particles produced during the initial phase of the collision (where hard interactions of incoming partons occurs) will then probe this state of matter [1,3].

Heavy quarks :

- Produced at the early stages of the collision through gluon fusion and $q\bar{q}$ annihilation.
 - Not affected by the chiral symmetry breaking.
 - Study of their energy loss through the medium as well as their collective flow.
- ⇒sensitive probe to test medium characteristics (thermalization).

•Studies using semi-leptonic decays does not provide the relative contributions of charm and bottom decays in the electron spectra.

Figure 1 : (left) B contribution to non-photonics electrons for p+p at 200 GeV [2]; (right) Nuclear modification factor R_{AA} for d+Au and Au+Au collisions at $\sqrt{s} = 200$ GeV [4].



→Need direct reconstruction of the topological decays

Technical design

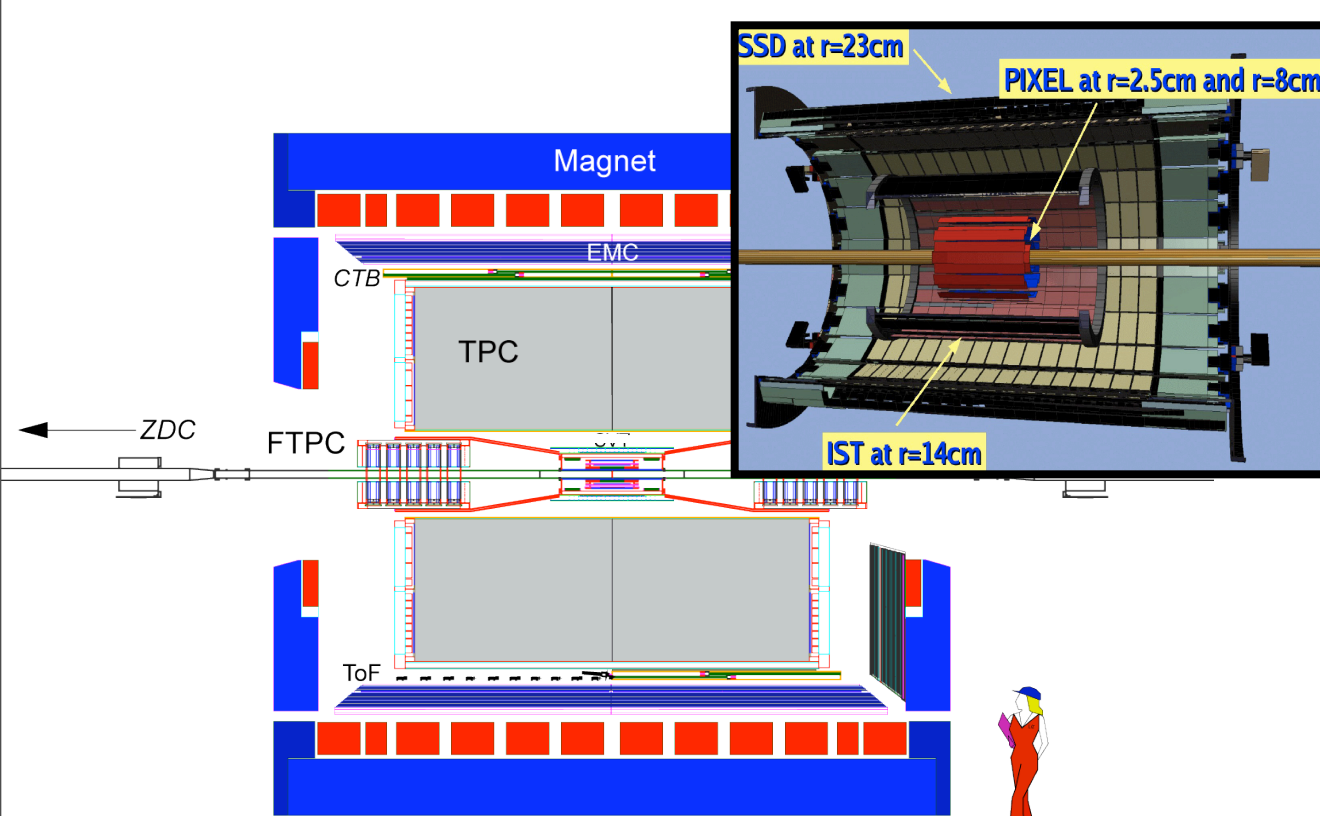


Figure 2: (left) Side view of STAR detector; (right) oblique view of the HFT showing the beam pipe surrounded by the 4 layers of silicon detectors.

To reach this goal, the STAR collaboration has proposed a micro-vertex detector composed by :

- The existing **SSD** : a single layer of silicon strips detector located at a radius of 23 cm from the beam axis.
- PIXEL** detector : The goal of this detector is to measure with great accuracy the track pointing resolution and to find secondary decays. It is made by 2 layers of 18.4 $\mu\text{m} \times 18.4 \mu\text{m}$ CMOS Active Pixel sensors [3].

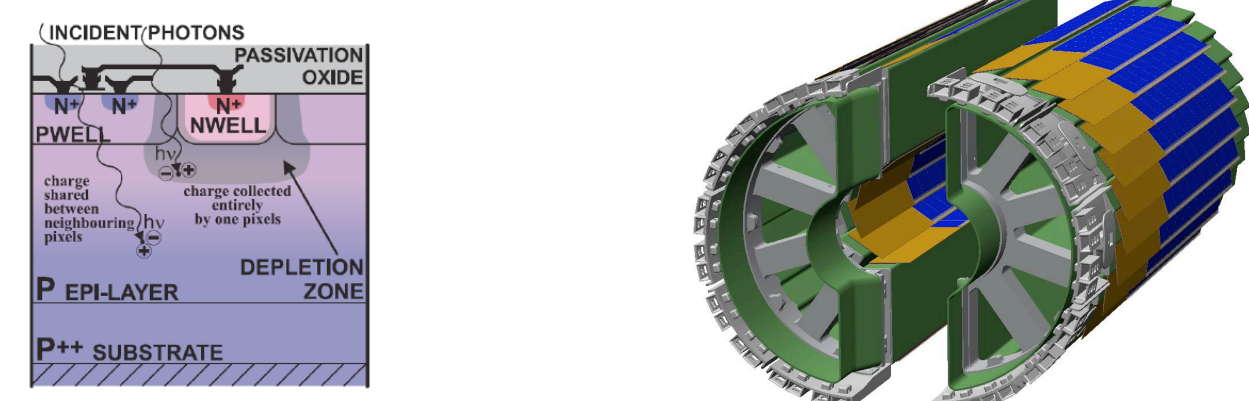


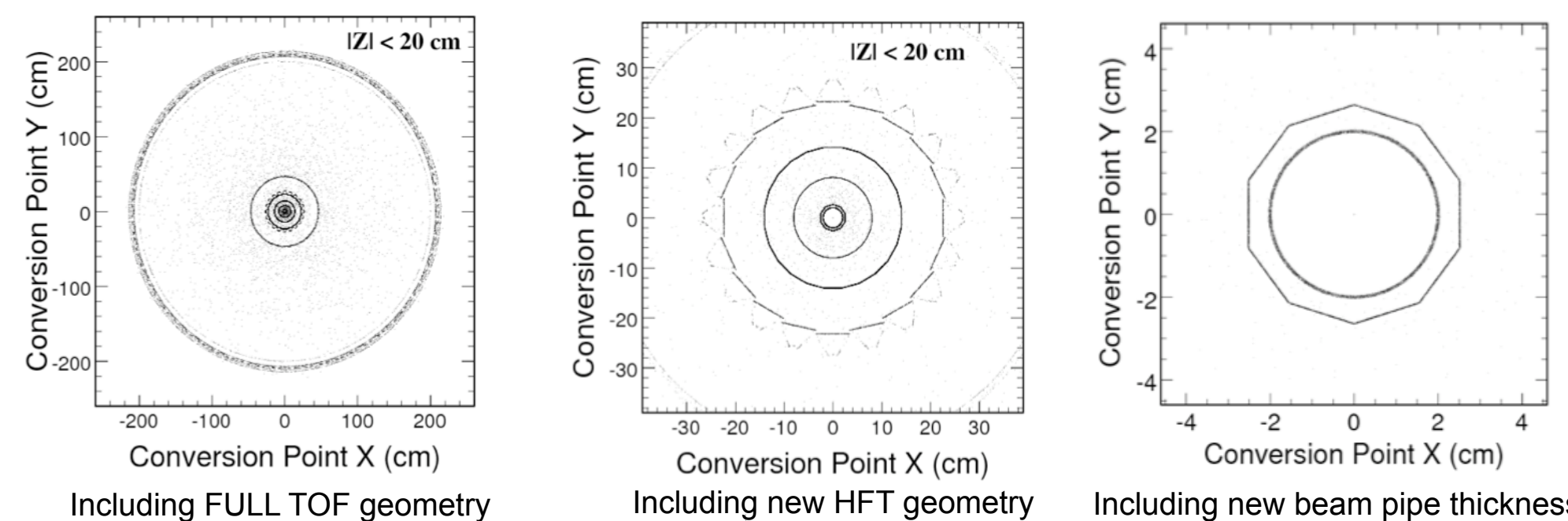
Figure 3: (left) Principle of CMOS sensors for particle detection; (right) Configuration of the 2 PIXEL layers; (bottom) Configuration of IST detector and details of 1 ladder.

•**IST** : 1 intermediate layer of single sided strips : it guides tracks from the SSD through PIXEL detector. It is composed of 24 liquid cooled ladders equipped with 6 silicon strip-pad sensors.

Direct Charm (D-meson) reconstruction

DETECTOR	RADIUS (cm)	HIT RESOLUTION $R_{\perp}(\mu - \mu)$ ($\mu\text{m} - \mu\text{m}$)	Radiation length
SSD	23	30 / 857	1% X_0
IST	14	170 / 1700	1.2% X_0
PIXEL	8	8.6 / 8.6	-0.3% X_0
	2.5	8.6 / 8.6	-0.3% X_0

Table 1 : Characteristics of each silicon layer involved in the simulation.



Including FULL TOF geometry

Including new HFT geometry

Including new beam pipe thickness

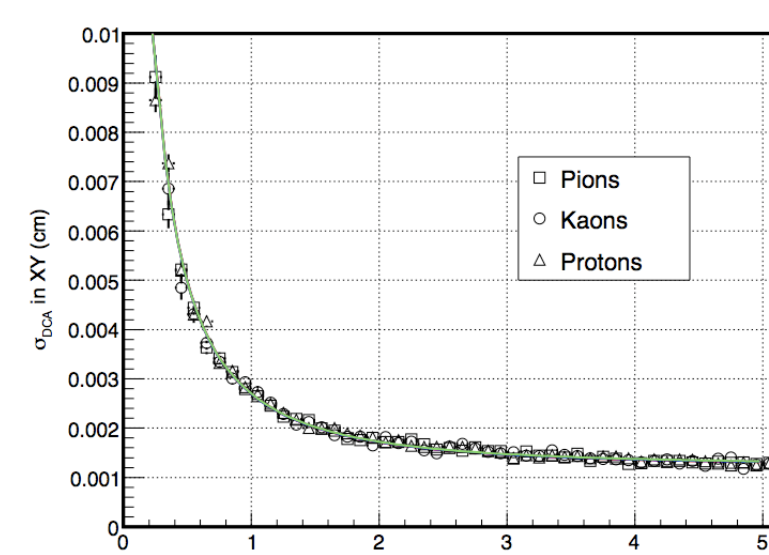


Figure 4 : Pointing resolution in r_{\perp} to primary vertex for single particles (of K, π^+, p) including all hits in HFT.

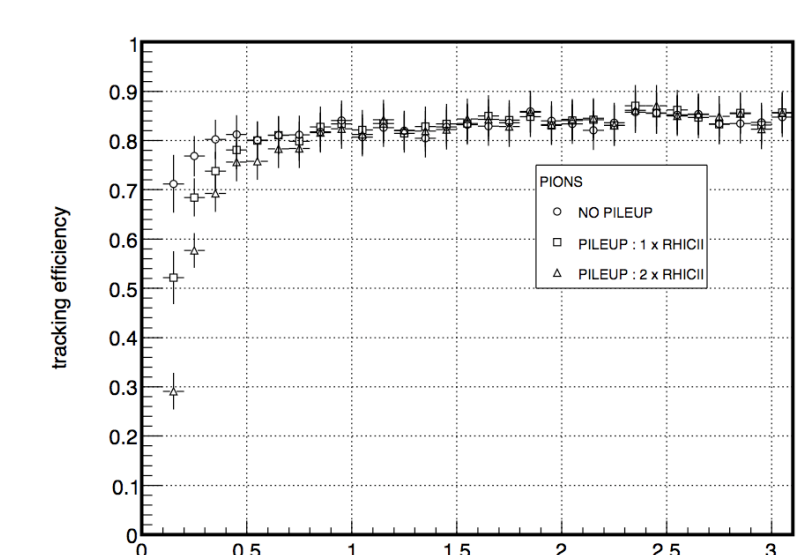


Figure 5 : Tracking efficiency of single π^+ for 3 pileup hits densities.

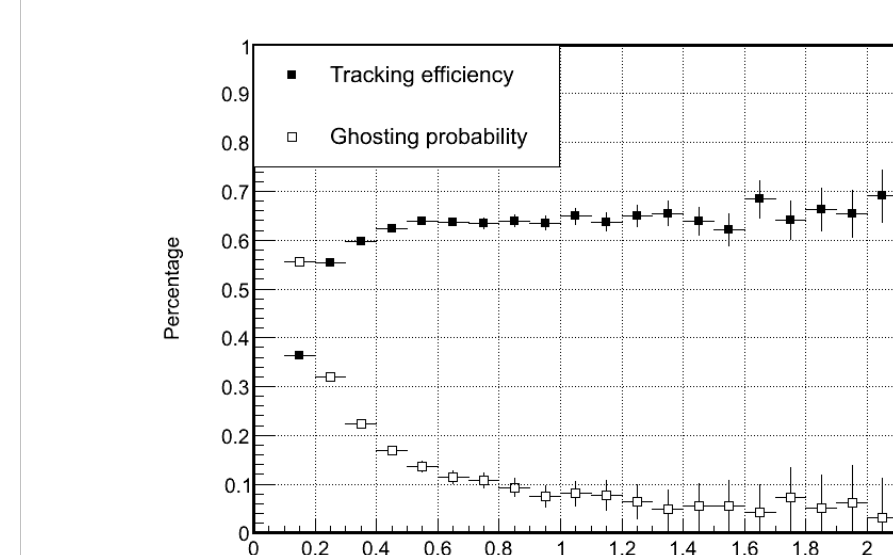


Figure 6 : Silicon Tracking inefficiency in central Au+Au events (see text below for details of simulations).

10k Au+Au events at 200 GeV embedded with $D^0, D_s, D_s^+, \Lambda_c$. Pseudo-random hits (pileup) effect taken into account in the PIXEL detector, corresponding to MinBias collision rate of 80 kHz (assuming RHIC-II luminosity). Tracking efficiency : requirement of 15 hits in TPC and 2 hits in PIXEL detector.

D^0 efficiency : based on PID identification and topological cuts applied to the daughters candidate (fig. 7 and tab. 2). Extended PID provided by TOF has been used.

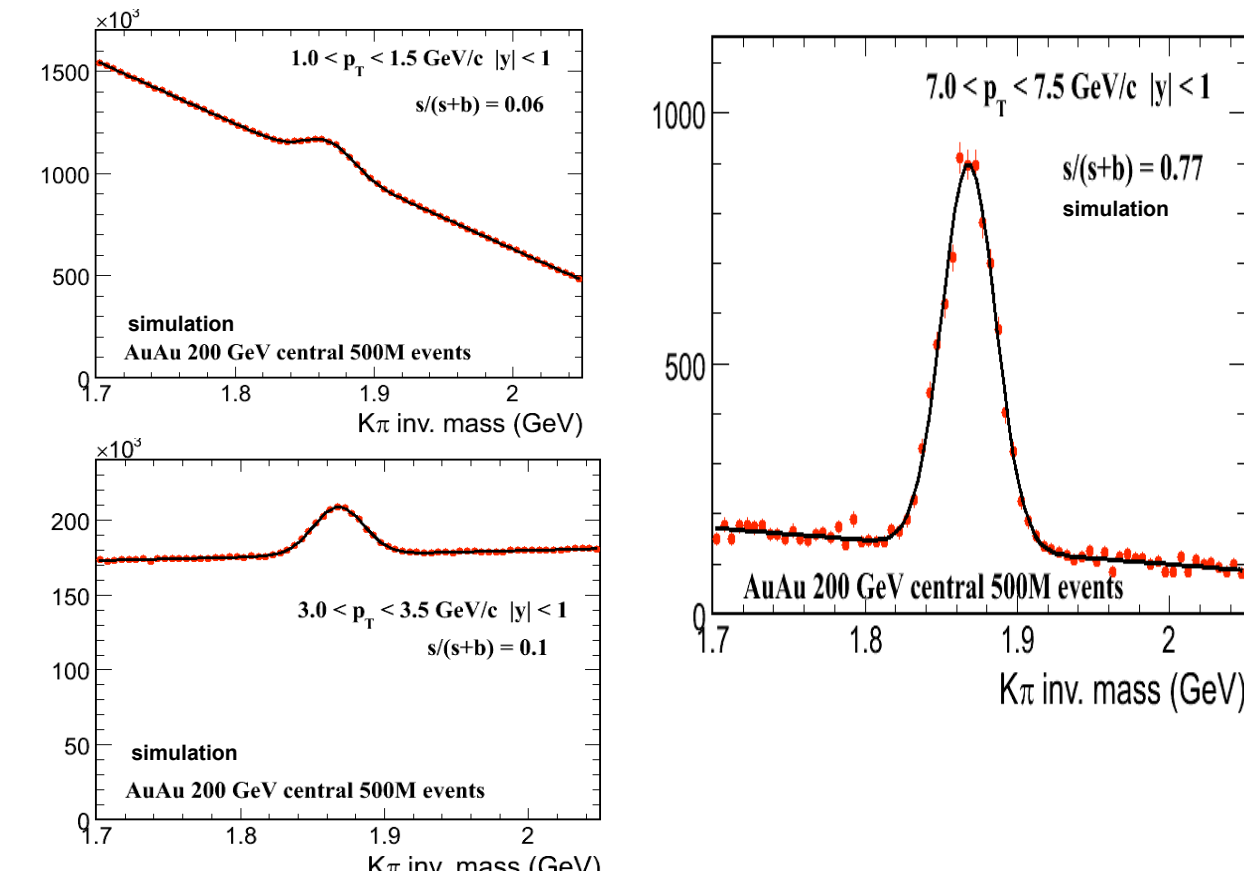


Figure 8 : (left) Invariant mass of D^0 's using TOF PID for 3 p_T bins. (right) Yield of reconstructed D^0 's over yield of simulated D^0 's before (squares) and after (circles) applying topological cuts (tab. 2). [open symbols are for the current geometry, compared to previous geometry studied].

Figure 7 : Topology of a D^0 decay into a kaon and pion.

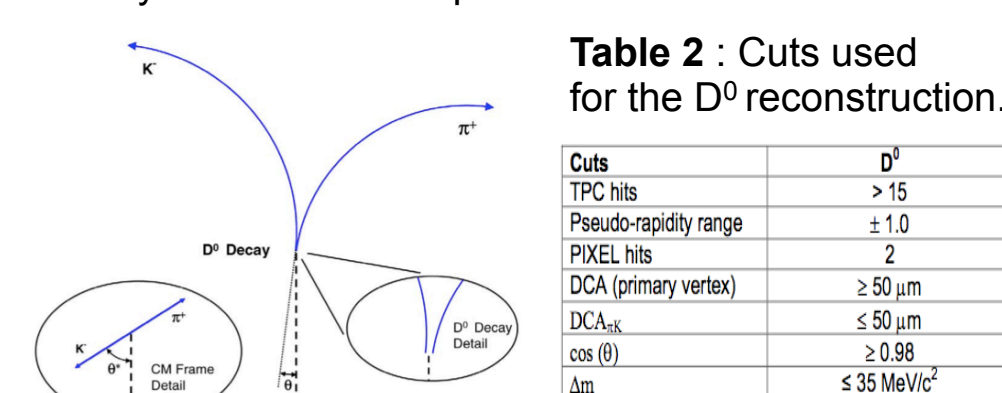
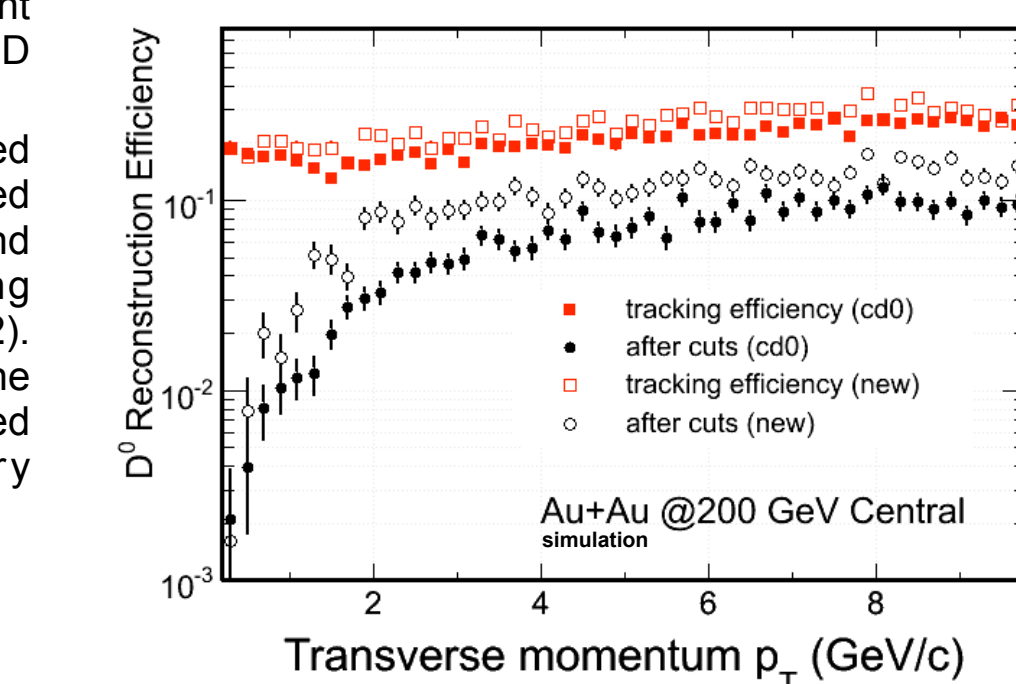


Table 2 : Cuts used for the D0 reconstruction.

Cuts	D^0
TPC hits	> 15
Pseudo-rapidity range	± 1.0
PIXEL hits	≥ 2
DCA (primary vertex)	$\geq 50 \mu\text{m}$
DCA _{sec}	$\leq 50 \mu\text{m}$
$\cos(\theta)$	≥ 0.98
$\cos(\theta)$	≤ 0.98
$\cos(\theta)$	$\leq 35 \text{ MeV}/c^2$



Λ_c reconstruction

In this section results about the v_2 of D^0 and Λ_c and their R_{cp} are provided (see [5] for details). The Λ_c/D^0 ratio may be enhanced, as well as for the baryon/meson ratio in the intermediate p_T region.

Details of simulation :

• $D^0 \rightarrow K\pi^+$ (BR 3.8%, $\tau = 122.9 \mu\text{s}$)

• $\Lambda_c \rightarrow K\pi^+p$ (BR 5.0%, $\tau = 59.9 \mu\text{s}$)

→ Embedded in HIJING central Au+Au events at 200 GeV and filtered through STAR detector response simulators.

• $K-\pi$ separation up to $p_T < 1.6 \text{ GeV}/c$.

•Topological cuts based on DCA of tracks to primary vertex ; Λ_c momentum vector pointing back to the primary vertex to remove background.

•Final cut on the reconstructed mass to be in $2.3 \text{ GeV}/c^2 < m_{inv} < 2.70 \text{ GeV}/c^2$.

•Daughters tracks required to have 2 PIXEL hits.

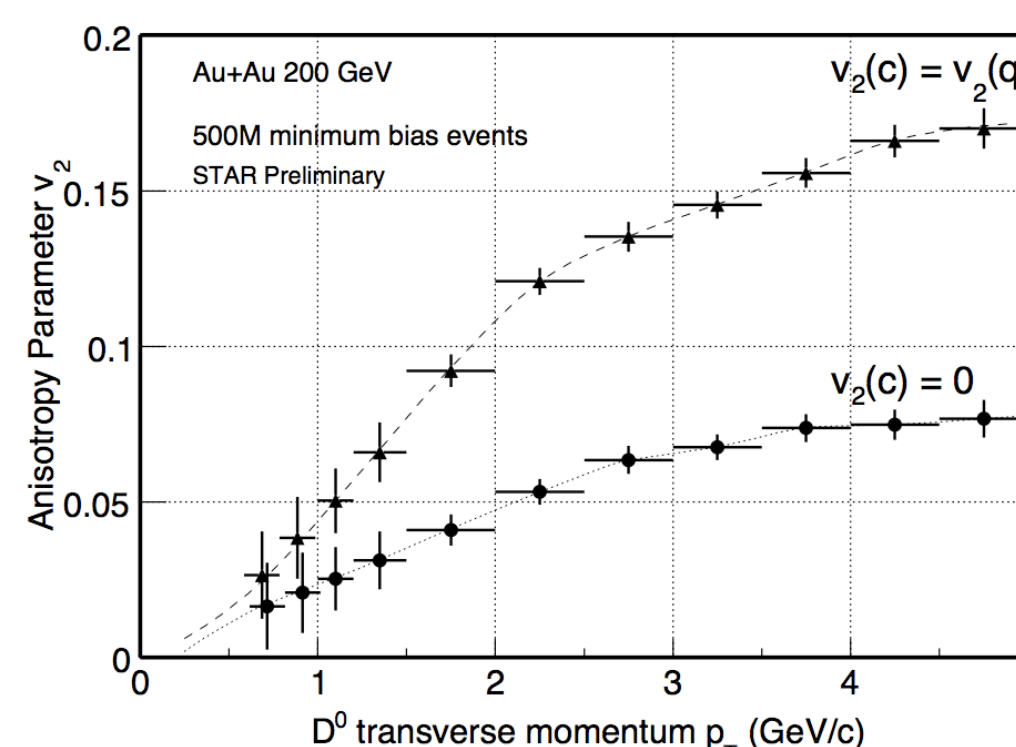


Figure 11 : v_2 of D^0 for 2 extremes elliptic flow models. Statistic of 500.10⁶ MinBias Au+Au is assumed, corresponding at 1 month of data collected by STAR.

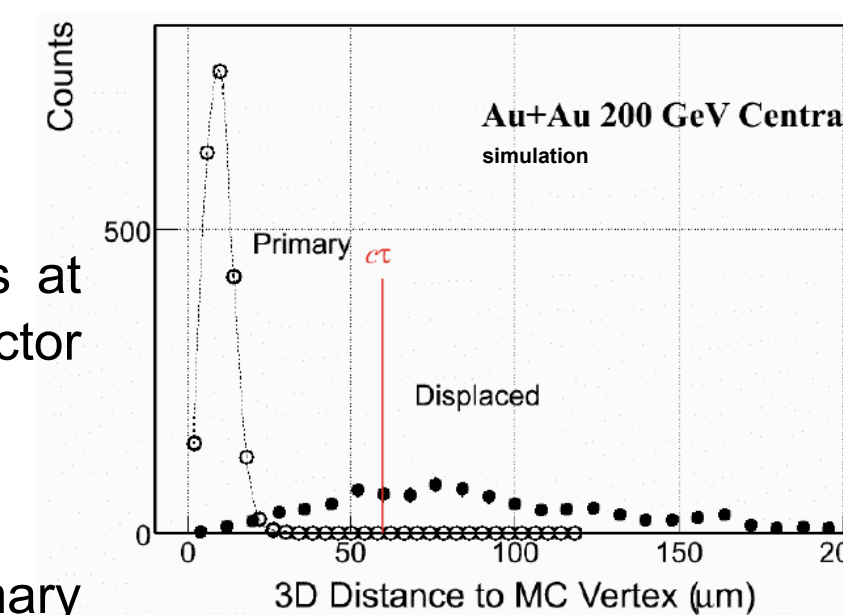


Figure 9 : Ability of the HFT to identify secondary vertices (in this plot from Λ_c symbolized by the red line) that are displaced from the primary vertex because of the separation by more their respective widths.

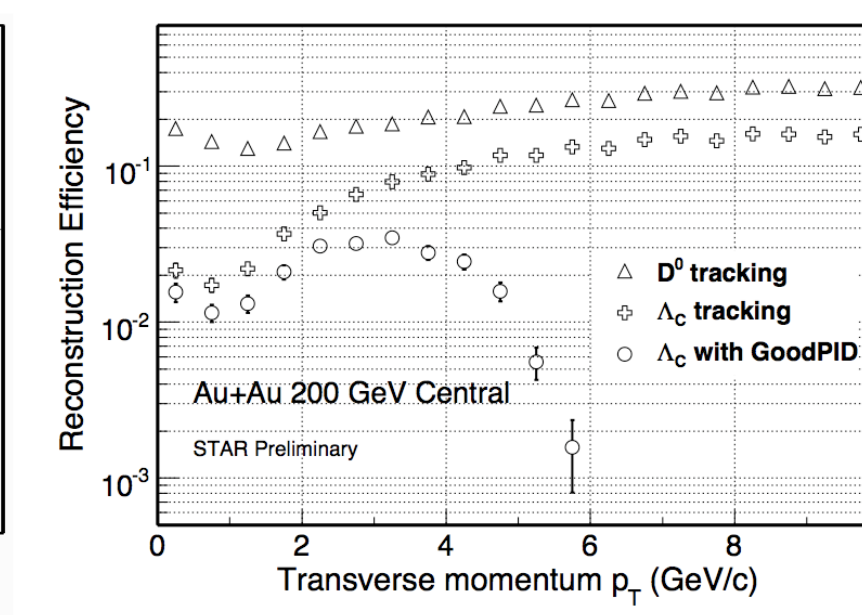


Figure 10 : Efficiency of D^0 and Λ_c reconstruction. Λ_c efficiency is lower than D^0 because of its 3 body decay. Detector acceptance also reduces the PID (open circles) cut.

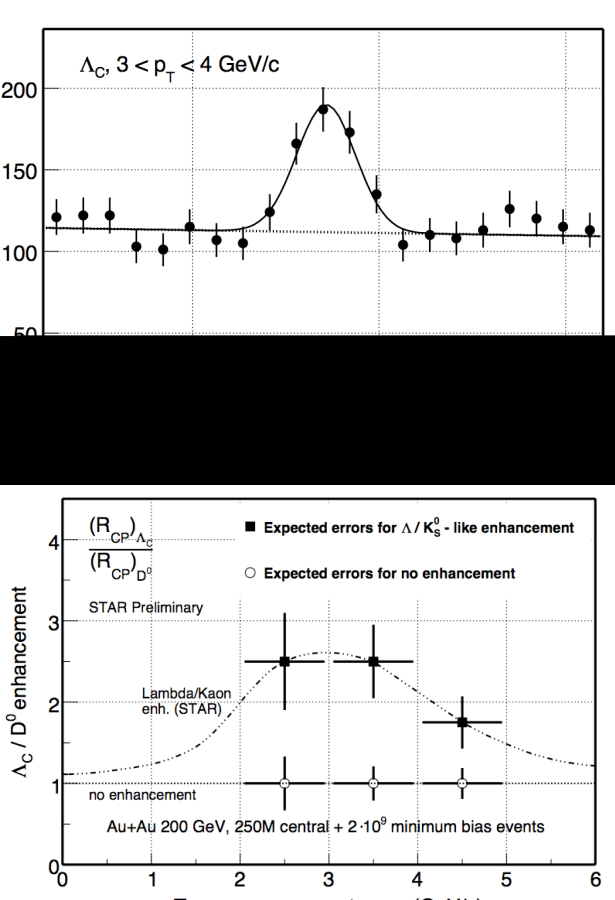
Figure 12 : (top) : Λ_c invariant mass distribution for $3 < p_T < 4 \text{ GeV}/c$.

→ Significance of 8 σ for 500.10⁶ central Au+Au events is expected.

(bottom) : expected Λ_c/D^0 ratio measurement. 2 scenarios are investigated :

•No enhancement and ratio flat equal to 0.2

•Enhancement equal to Λ/K_s^0
→ Statistical errors are well distinguished making a measurement of baryon/meson ratio in charm sector with good precision in HI collisions.



B meson measurement

B meson measurement via their semi-leptonic was done according to 2 methods :

Impact parameter method (as used by ALICE collaboration) to separate electrons of B decays from those of D decays. Because of the electrons from B have greater impact parameter d_0 , a cut using the resolution achieved by the HFT based on a minimal value of d_0 is possible. In this study B^+ and D^+ are embedded in HIJING central events Au+Au collisions at 200 GeV. The spectra of non-photonics electrons spectra after STAR data reconstruction is measured (fig. 11). As it is seen on fig. 13 (left), there is a **clear region for $4 < p_T < 5 \text{ GeV}/c$** where the electrons from B decays dominate ; their spectra and comparison to electrons from D are represented on fig. 13 (right).

Displaced vertices to measure contribution of electrons from indirect ($B \rightarrow J/\Psi \rightarrow e^+e^-$) and direct $J/\Psi (J/\Psi \rightarrow e^+e^-)$. This method uses a cut on the pseudo- τ defined as :

$$\tau = \vec{L} \cdot \frac{p_T^{\Psi} M_{\Psi}}{|p_T^{\Psi}| \Psi \cdot \frac{M_{\Psi}}{p_{\Psi}}}$$

Pythia J/Ψ 's are embedded in central Au+Au collisions from HIJING.

Fig 13 : (left) Impact parameter distributions of electrons from B and decays; (right) electrons yield for 200 $\mu\text{m} < d_0 < 600 \mu\text{m}$ and $p_T > 4 \text{ GeV}/c$.

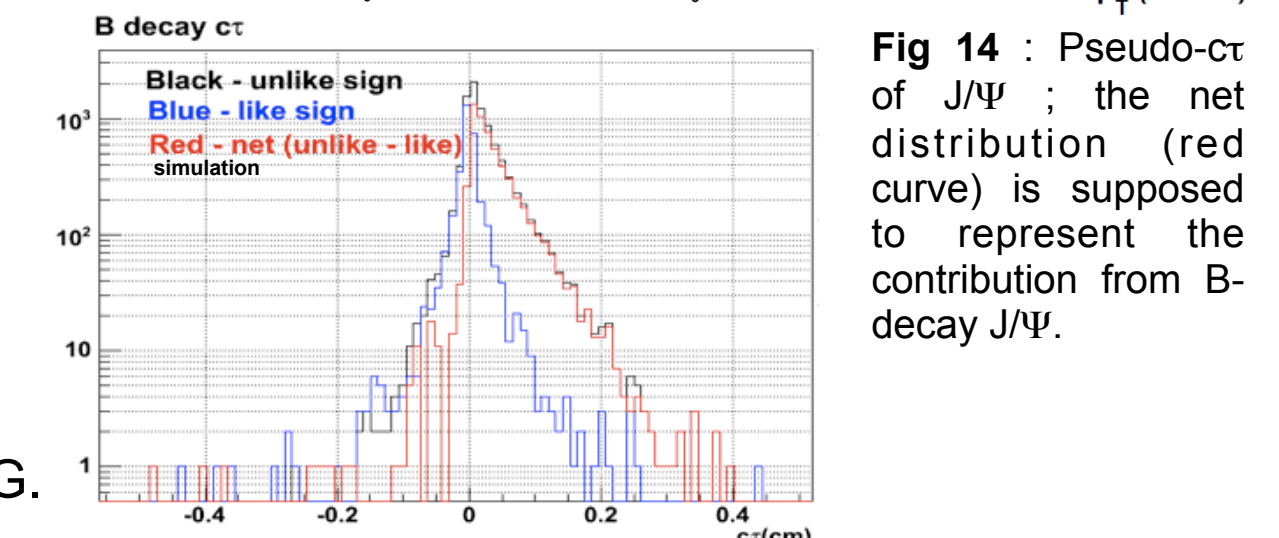
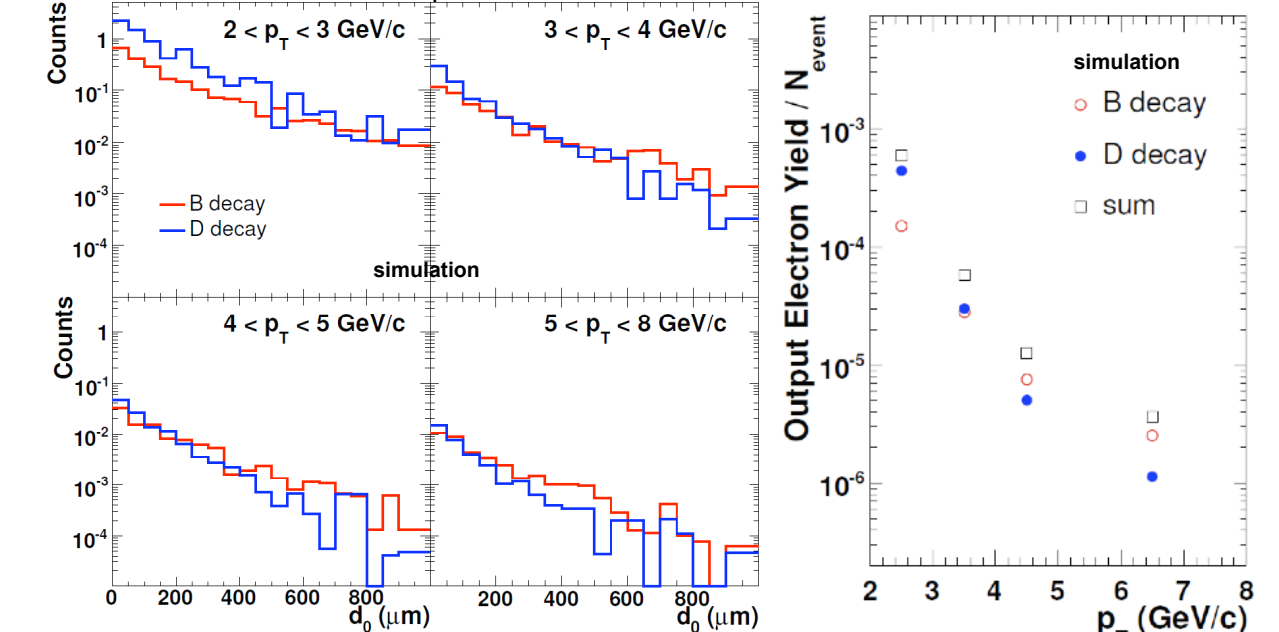


Figure 14 : Pseudo- τ of J/Ψ ; the net distribution (red curve) is supposed to represent the contribution from B-decay J/Ψ .

A realistic simulator

• Calculate the number of electrons generated from charged tracks through the silicon sensor using a Bichsel distribution.

• Build the geometry of the detector : 1 chip made of 640 30 $\mu\text{m} \times 50 \mu\text{m} \times 30 \mu\text{m}$ pixels composed by different layers (readout electronics, substrate and active layers).

• Simulate the transportation of electrons :
1. Diffusion, recombination and reflection at the interfaces between layers.
2. Recalculate the number of electrons collected.

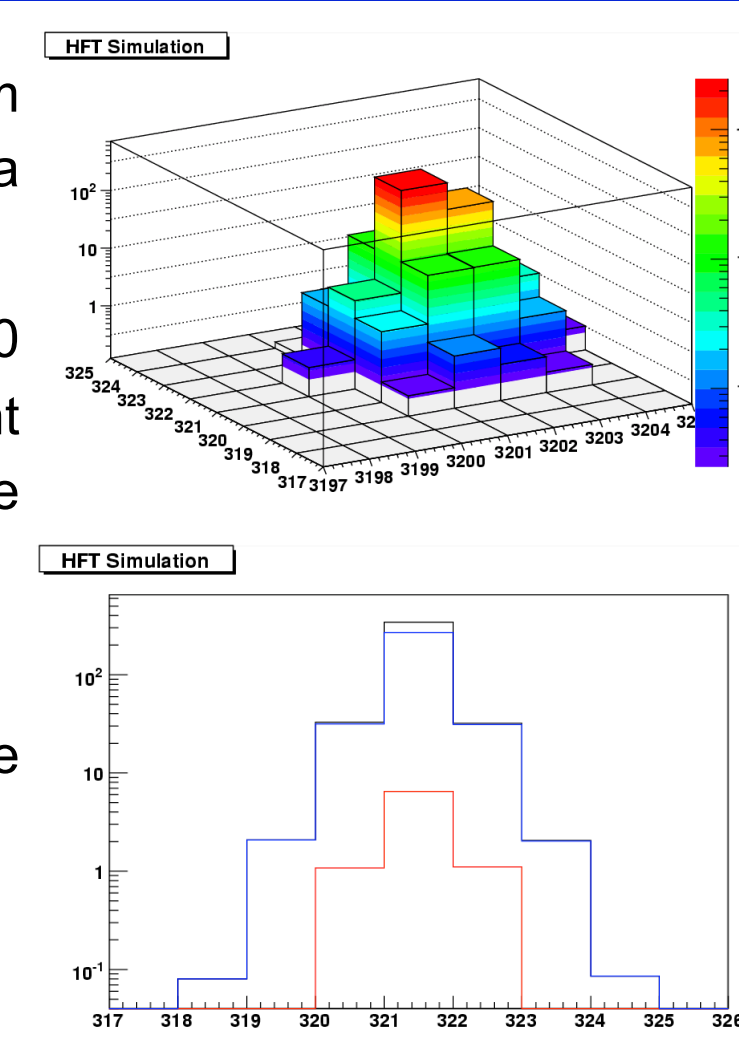


Figure 15 : (left) Reconstructed cluster profile of electrons deposited from a single track with incident angle = 45°.

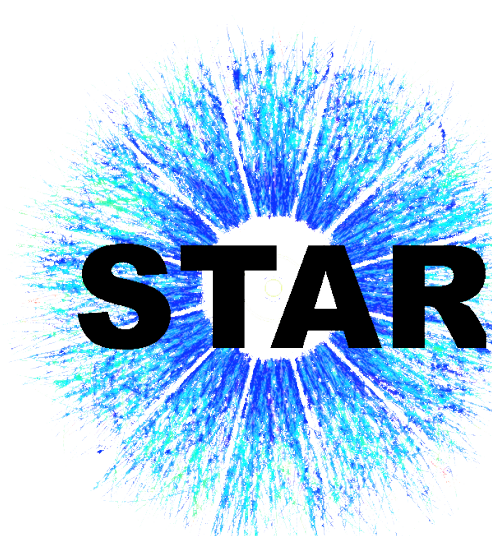
Figure 16 : (left) Distribution of the number of electrons collected by fired pixel and its neighbors and the number of electrons collected by the epitaxial layer and substrate layers. The contribution from the epitaxial layer is 81.7% and from the substrate layer : 2.1%.

Summary

- The HFT will be able to reconstruct direct charm and bottom hadrons.
- Pixel detector using low-mass CMOS sensors to minimize Multiple Coulomb Scattering.
- Confirmation of the performances (pointing resolution, tracking efficiency) with Monte-Carlo Simulations of Au+Au collisions at 200 GeV including STAR detector response simulators.
- Improvement of measurement B meson.

1. Z. Lin and M.Gyulassy, phys. Rev. C77 (1996)1222
2. G. Wang, J. Phys. G : Nucl. Part. Phys. 35 (2008) 104107
3. E. Anderssen et al., A Heavy Flavor Tracker for STAR (http://mc.lbl.gov/hft/docs/hft_final_submission_version.pdf)
4. B. Abelev et al., Phys. Rev. Lett 98 192301 (2007)
5. J. Kapitan, STAR inner tracking upgrade - A performance study, proceeding of HotQuarks 2008





Heavy Flavor Tracker (HFT) : a new inner tracking device at STAR

Jonathan Bouchet¹, for the STAR collaboration

¹ Kent State University, Ohio, USA



Abstract

Due to their large masses, heavy flavor (c and b quarks) are produced in the early stages of heavy ion collision [1]. The measurement of charm meson nuclear modification factor R_{AA} , as well as their flow velocity will be investigated by the HFT. A precise measurement of heavy flavor production could be achieved by identifying the decay of charm meson using direct topological reconstruction and thus disentangling the b and c quarks. The HFT is a proposed new inner tracking detector for STAR.

Introduction : the physics of HFT

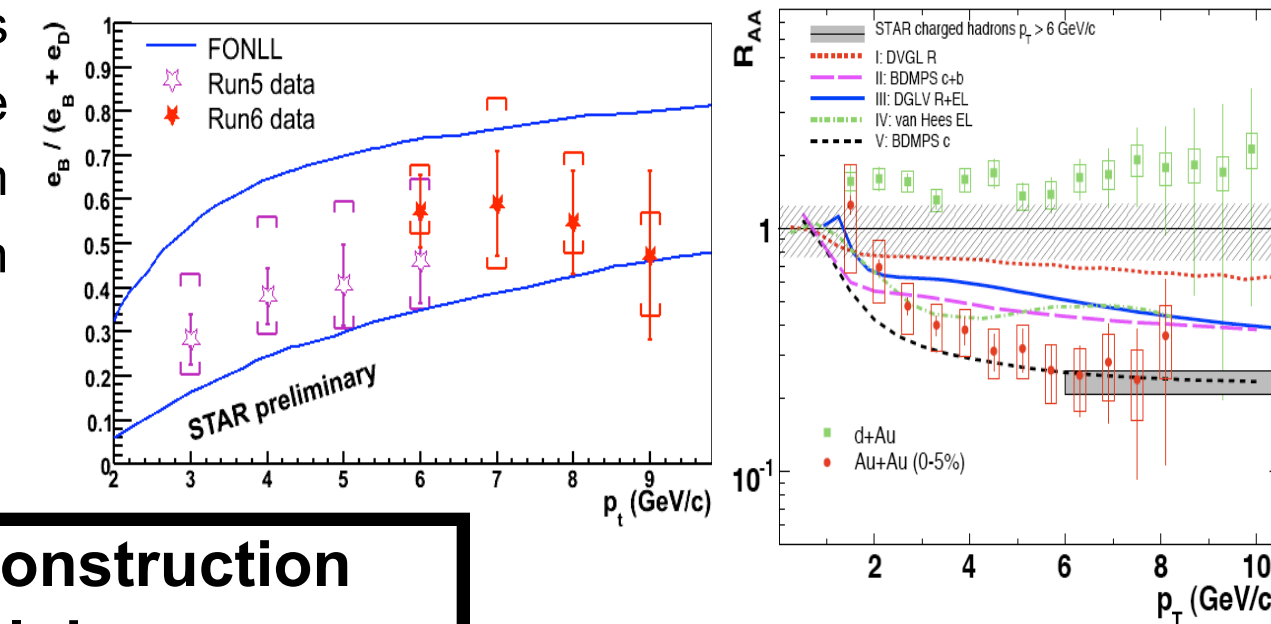
The studies of high energies collisions occurred RHIC are supposed to give insights about the nuclear matter at extreme temperatures and energy densities and describe the so-called Quark-Gluon Plasma. Investigation of particles produced during the initial phase of the collision (where hard interactions of incoming partons occurs) will then probe this state of matter [1,3].

Heavy quarks :

- Produced at the early stages of the collision through gluon fusion and $q\bar{q}$ annihilation.
- Not affected by the chiral symmetry breaking.
- Study of their energy loss through the medium as well as their collective flow.
- sensitive probe to test medium characteristics (thermalization).

Studies using semi-leptonic decays does not provide the relative contributions of charm and bottom decays in the electron spectra.

Figure 1 : (left) B contribution to non-photonics electrons for p+p at 200 GeV [2]; (right) Nuclear modification factor R_{AA} for d+Au and Au+Au collisions at $\sqrt{s} = 200$ GeV [4].



→ Need direct reconstruction of the topological decays

Technical design

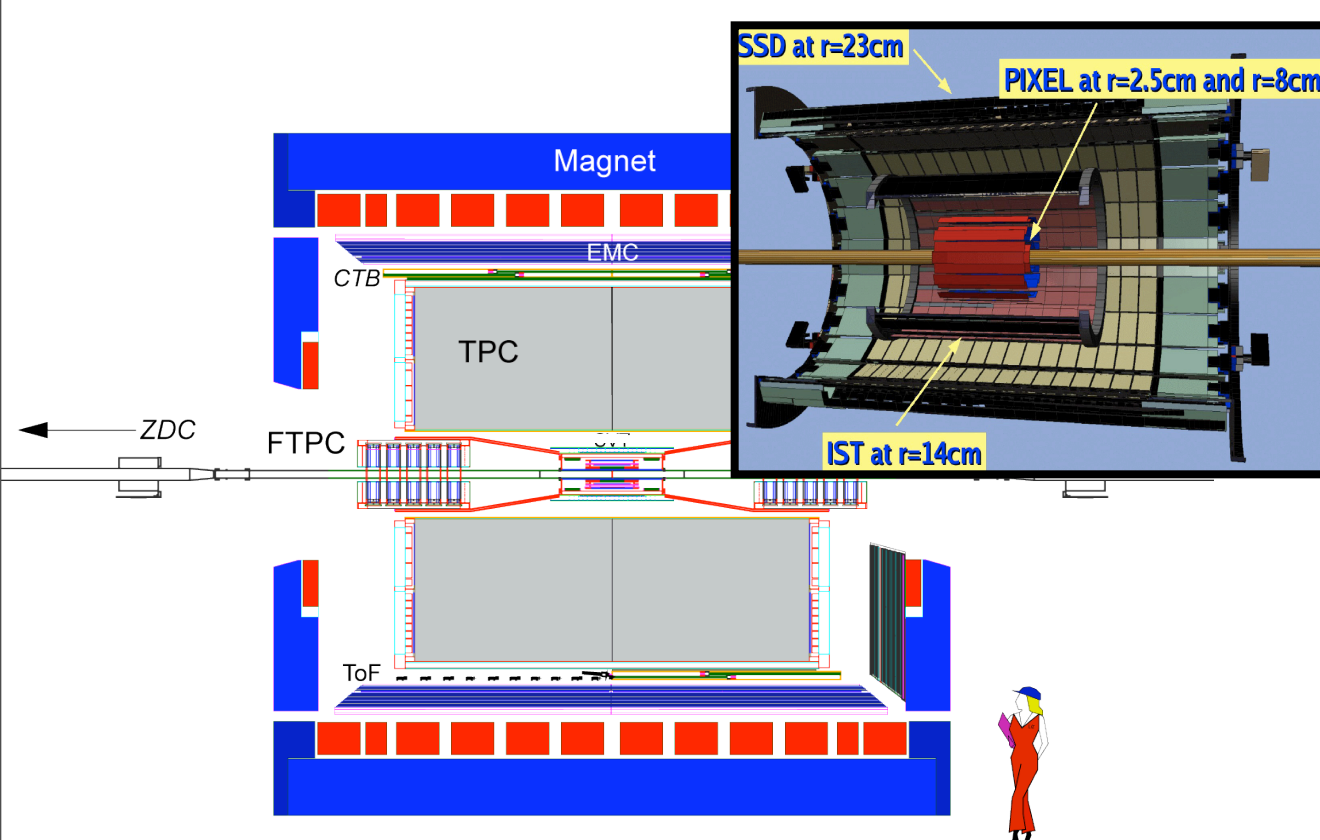


Figure 2: (left) Side view of STAR detector; (right) oblique view of the HFT showing the beam pipe surrounded by the 4 layers of silicon detectors.

To reach this goal, the STAR collaboration has proposed a micro-vertex detector composed by :

- The existing SSD : a single layer of silicon strips detector located at a radius of 23 cm from the beam axis.
- PIXEL detector : The goal of this detector is to measure with great accuracy the track pointing resolution and to find secondary decays. It is made by 2 layers of 18.4 $\mu\text{m} \times 18.4 \mu\text{m}$ CMOS Active Pixel sensors [3].

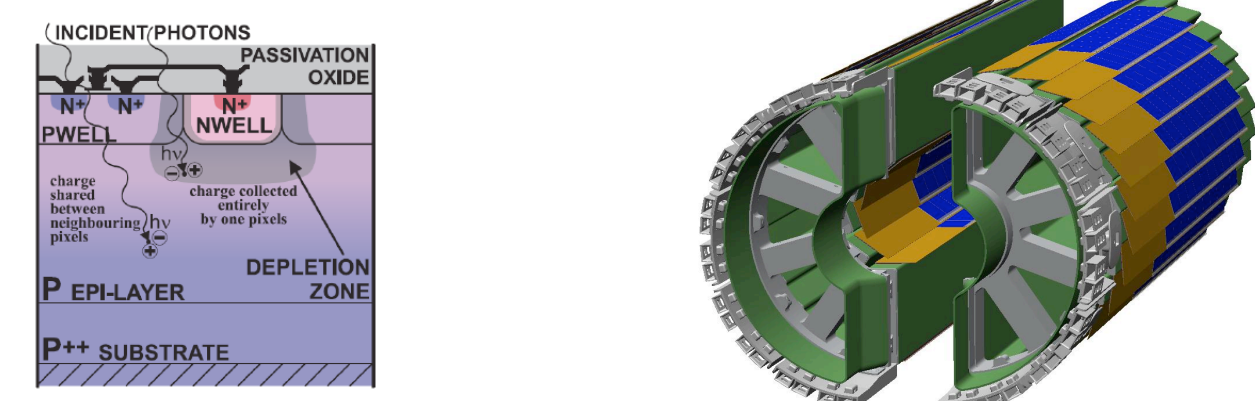


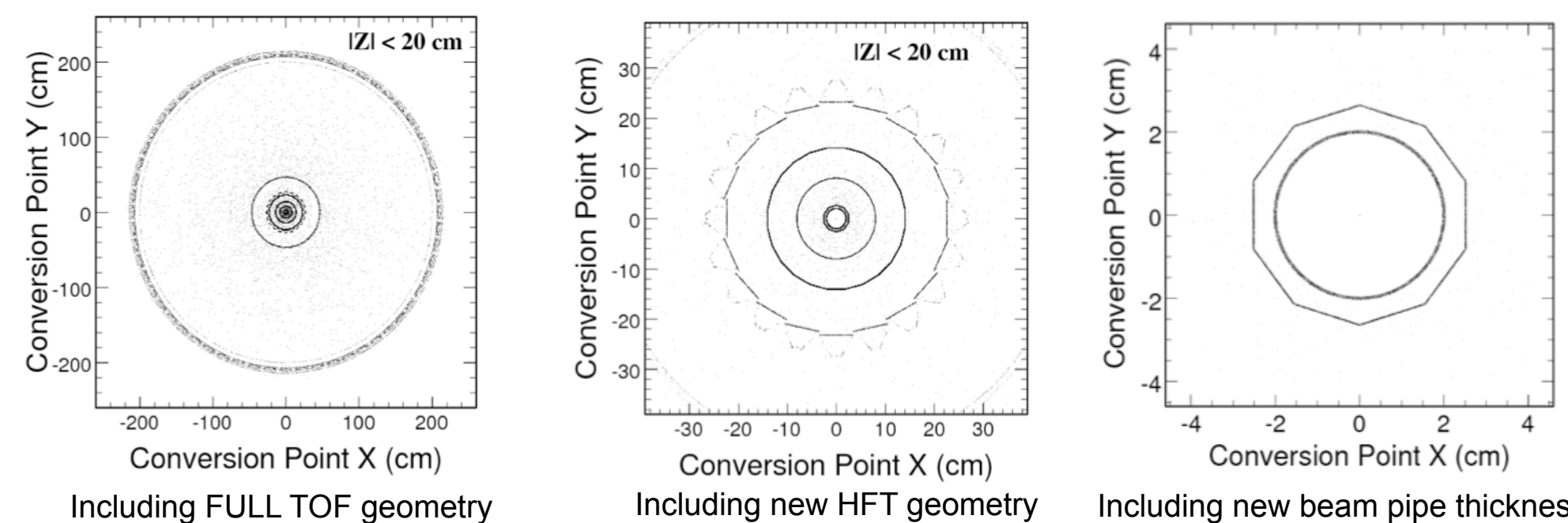
Figure 3: (left) Principle of CMOS sensors for particle detection; (right) Configuration of the 2 PIXEL layers; (bottom) Configuration of IST detector and details of 1 ladder.

IST : 1 intermediate layer of single sided strips : it guides tracks from the SSD through PIXEL detector. It is composed of 24 liquid cooled ladders equipped with 6 silicon strip-pad sensors.

Direct Charm (D-meson) reconstruction

DETECTOR	RADIUS (cm)	HIT RESOLUTION $R_{\perp}(\varphi - Z)$ ($\mu\text{m} - \mu\text{m}$)	Radiation length
SSD	23	30 / 857	1% X_0
IST	14	170 / 1700	1.2% X_0
PIXEL	8	8.6 / 8.6	-0.3% X_0
	2.5	8.6 / 8.6	-0.3% X_0

Table 1 : Characteristics of each silicon layer involved in the simulation.



Including FULL TOF geometry

Including new HFT geometry

Including new beam pipe thickness

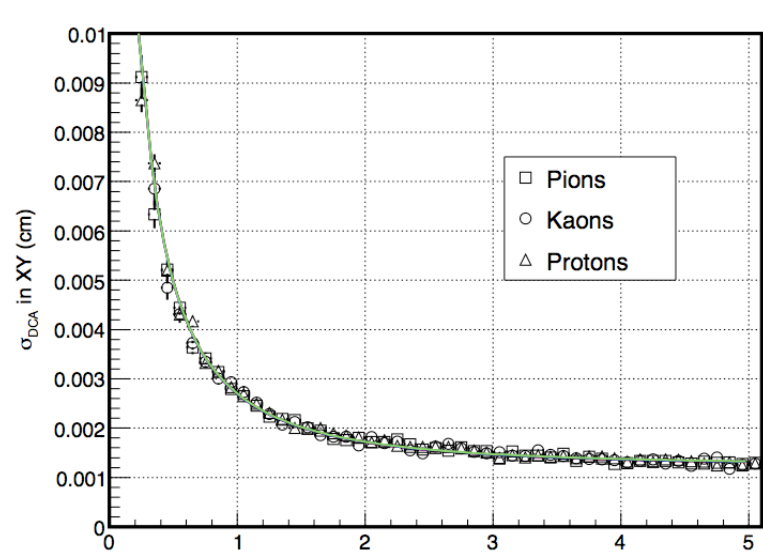


Figure 4 : Pointing resolution in $r-\varphi$ to primary vertex for single particles (of K, π^+, p) including all hits in HFT.

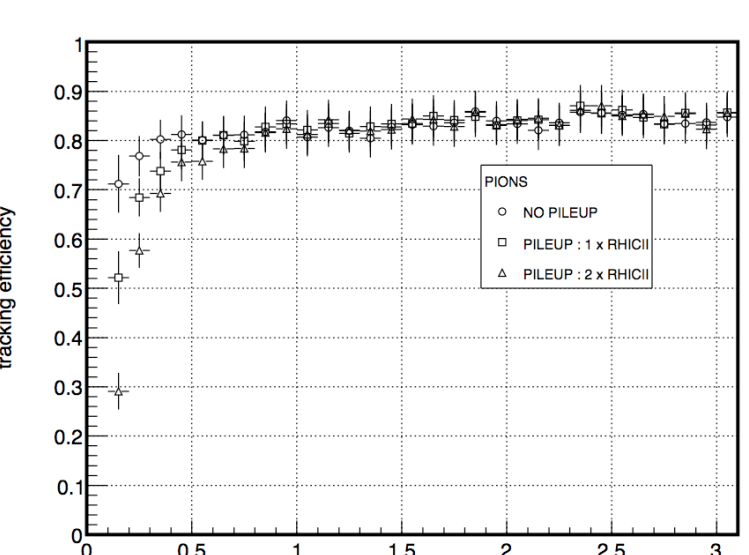


Figure 5 : Tracking efficiency of single π^+ for 3 pileup hits densities.

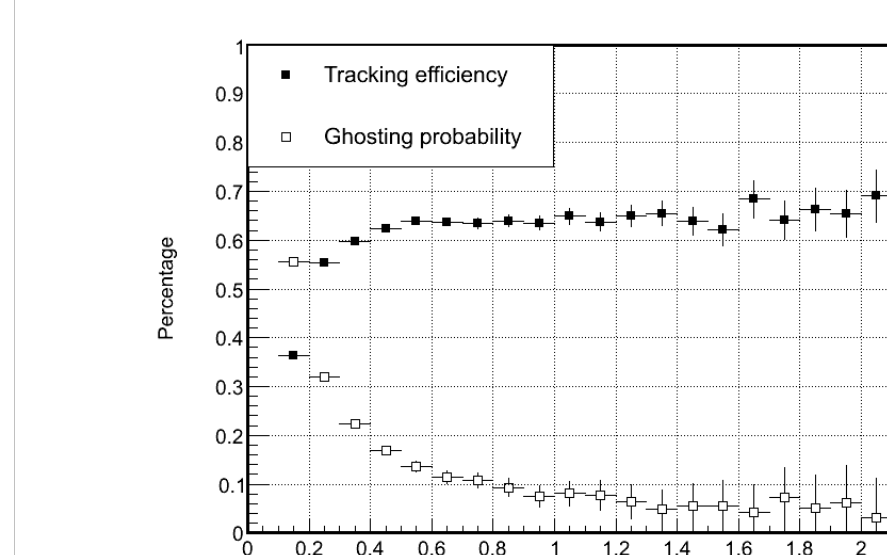


Figure 6 : Silicon Tracking inefficiency in central Au+Au events (see text below for details of simulations).

Figure 7 : Topology of a D0 decay into a kaon and pion.

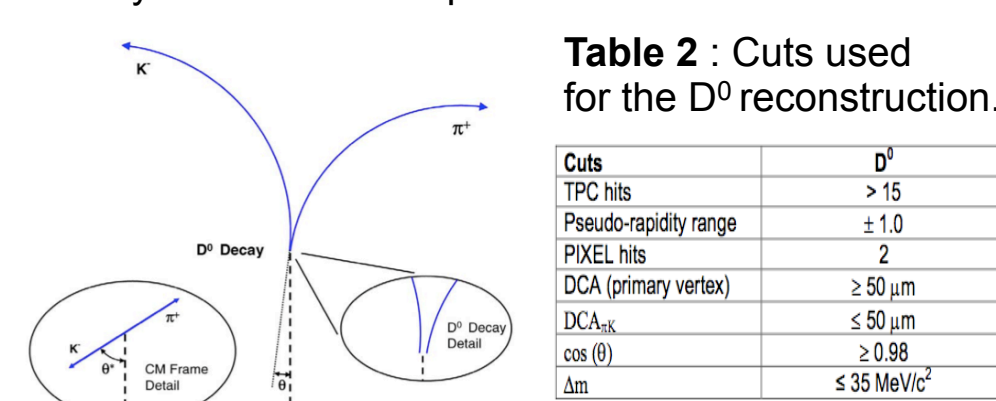


Table 2 : Cuts used for the D0 reconstruction.

Cuts	D0
TPC hits	> 15
Pseudo-rapidity range	± 1.0
PIXEL hits	≥ 2
DCA (primary vertex)	$\geq 50 \mu\text{m}$
DCA _{sec}	$\leq 50 \mu\text{m}$
cos(θ)	≥ 0.98
cos(θ)	≤ 0.98
cos(θ)	≤ 0.98

10k Au+Au events at 200 GeV embedded with $D^0, D_s, D_s^+, \Lambda_c$. Pseudo-random hits (pileup) effect taken into account in the PIXEL detector, corresponding to MinBias collision rate of 80 kHz (assuming RHIC-II luminosity).

Tracking efficiency : requirement of 15 hits in TPC and 2 hits in PIXEL detector.

D^0 efficiency : based on PID identification and topological cuts applied to the daughters candidate (fig. 7 and tab. 2). Extended PID provided by TOF has been used.

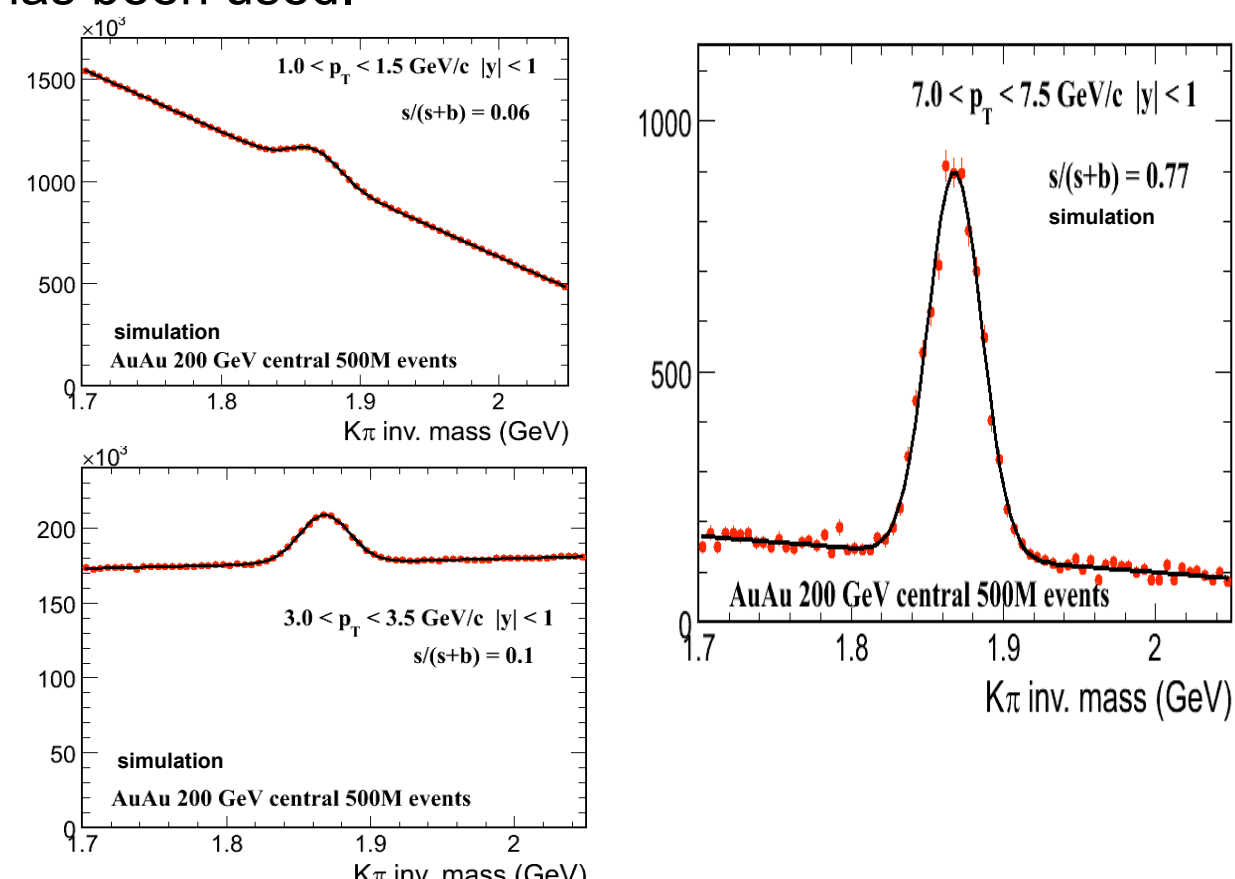
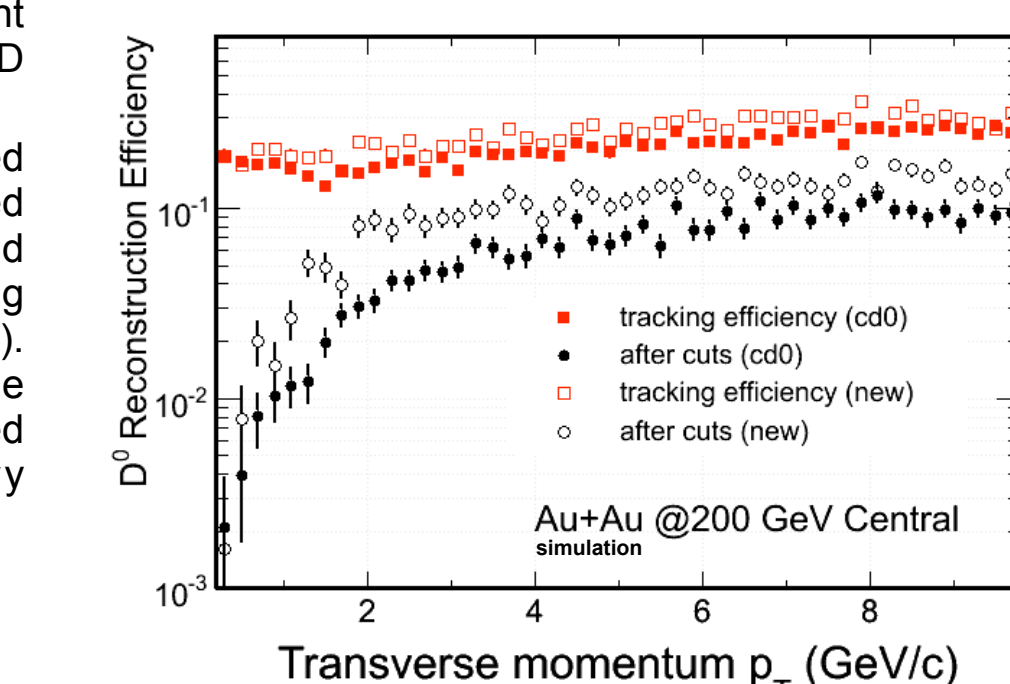


Figure 8 : (left) Invariant mass of D^0 s using TOF PID for 3 p_T bins. (right) Yield of reconstructed D^0 s over yield of simulated D^0 s before (squares) and after (circles) applying topological cuts (tab. 2). [open symbols are for the current geometry, compared to previous geometry studied].



Λ_c reconstruction

In this section results about the v_2 of D^0 and Λ_c and their R_{cp} are provided (see [5] for details). The Λ_c/D^0 ratio may be enhanced, as well as for the baryon/meson ratio in the intermediate p_T region.

Details of simulation :

$D^0 \rightarrow K\pi^+$ (BR 3.8%, $\tau = 122.9 \mu\text{s}$)

$\Lambda_c \rightarrow K\pi^+p$ (BR 5.0%, $\tau = 59.9 \mu\text{s}$)

→ Embedded in HIJING central Au+Au events at 200 GeV and filtered through STAR detector response simulators.

$K-\pi$ separation up to $p_T < 1.6$ GeV/c.

Topological cuts based on DCA of tracks to primary vertex ; Λ_c momentum vector pointing back to the primary vertex to remove background.

Final cut on the reconstructed mass to be in $2.3 \text{ GeV}/c^2 < m_{inv} < 2.70 \text{ GeV}/c^2$.

Daughters tracks required to have 2 PIXEL hits.

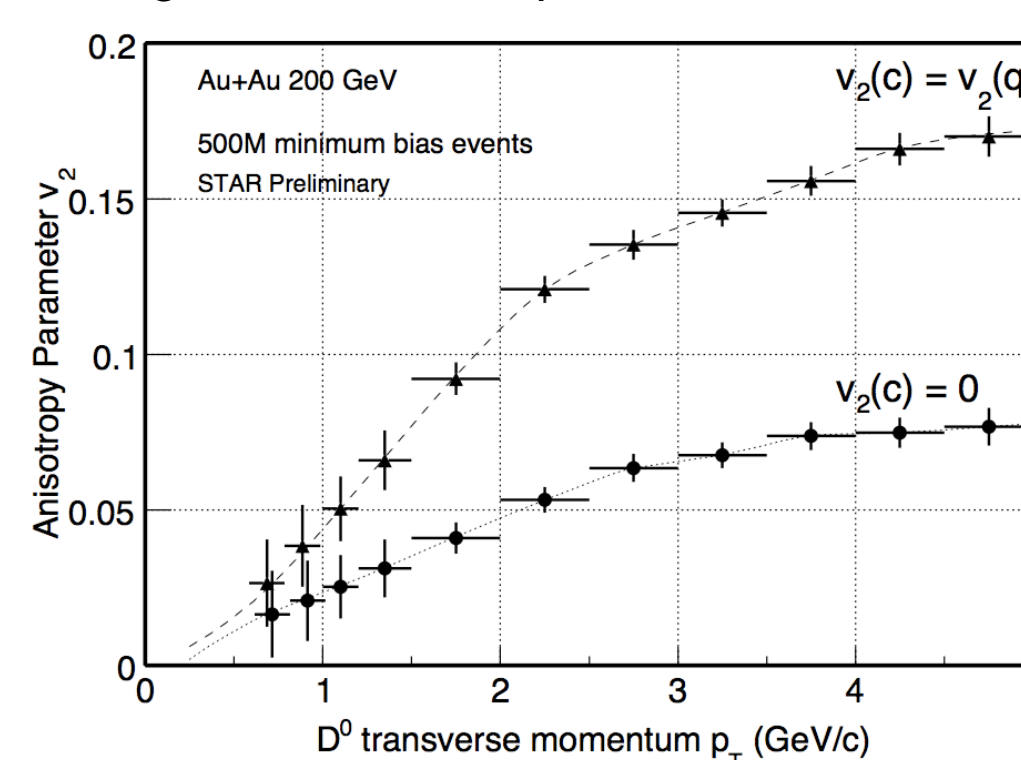


Figure 11 : v_2 of D^0 for 2 extremes elliptic flow models. Statistic of 500.10⁶ MinBias Au+Au is assumed, corresponding at 1 month of data collected by STAR.

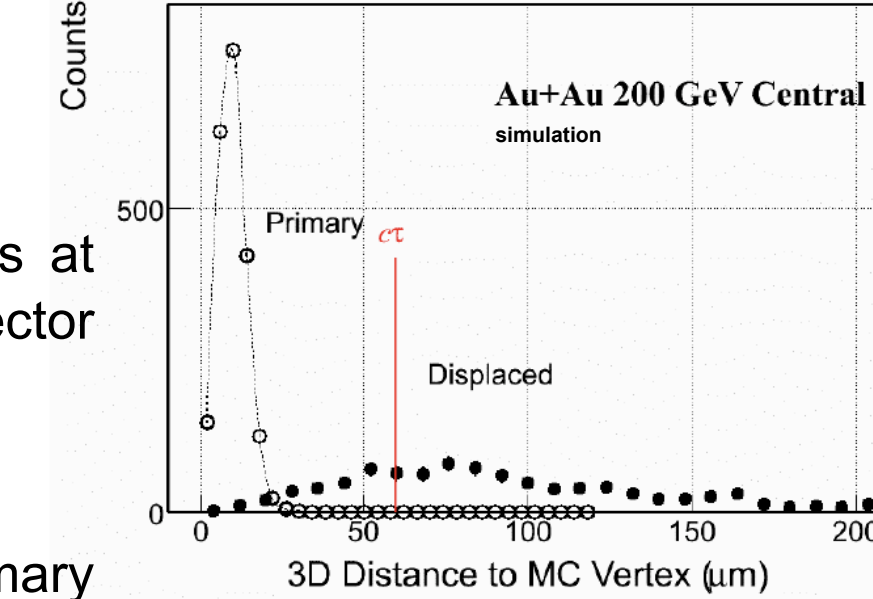


Figure 9 : Ability of the HFT to identify secondary vertices (in this plot from Λ_c symbolized by the red line) that are displaced from the primary vertex because of the separation by more their respective widths.

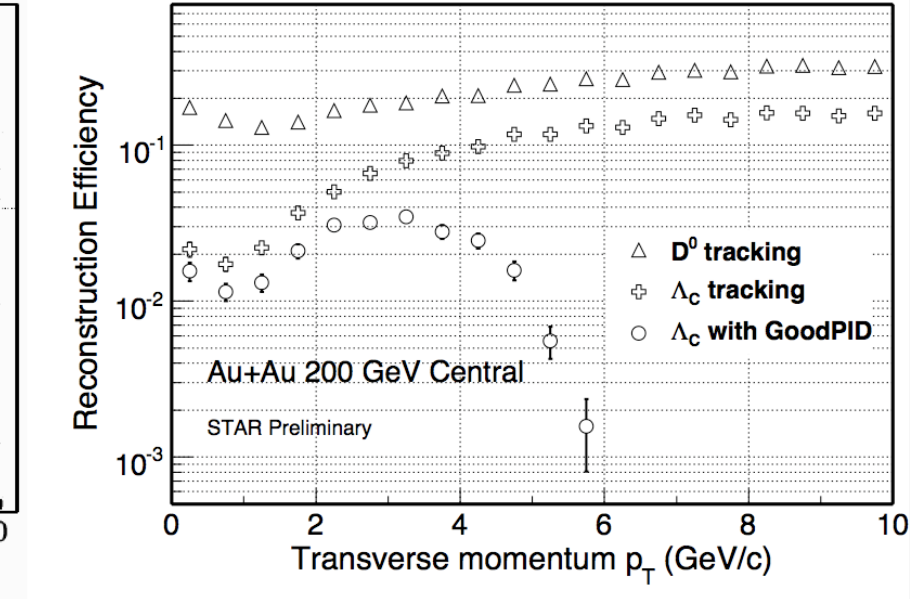


Figure 10 : Efficiency of D^0 and Λ_c reconstruction. Λ_c efficiency is lower than D^0 because of its 3 body decay. Detector acceptance also reduces the PID (open circles) cut.

Figure 12 : (top) : Λ_c invariant mass distribution for $3 < p_T < 4$ GeV/c.

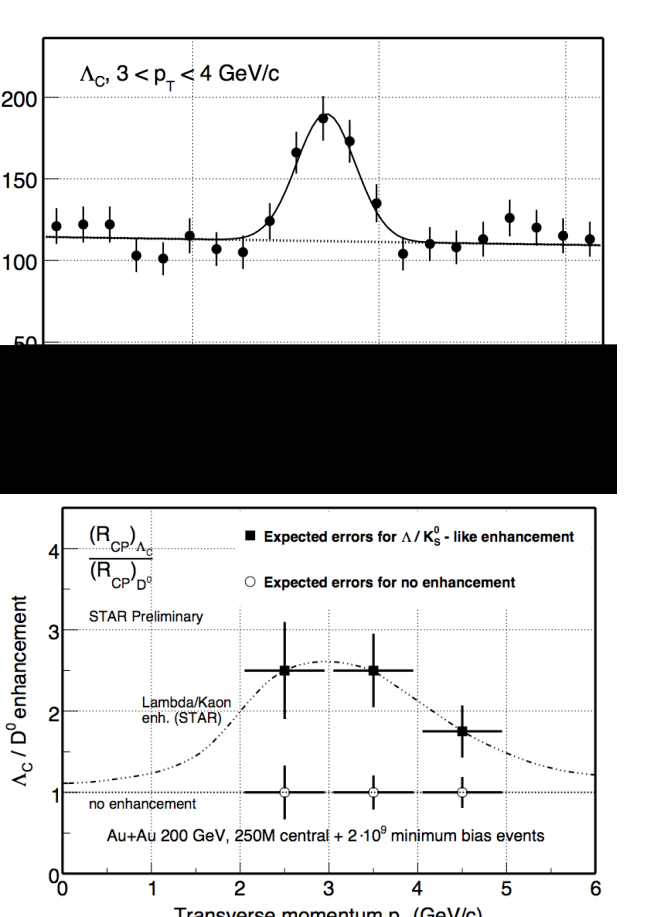
→ Significance of 8σ for 500.10⁶ central Au+Au events is expected.

(bottom) : expected Λ_c/D^0 ratio measurement. 2 scenarios are investigated :

No enhancement and ratio flat equal to 0.2

Enhancement equal to Λ/K_s^0

→ Statistical errors are well distinguished making a measurement of baryon/meson ratio in charm sector with good precision in HI collisions.



B meson measurement

B meson measurement via their semi-leptonic was done according to 2 methods :

Impact parameter method (as used by ALICE collaboration) to separate electrons of B decays from those of D decays. Because of the electrons from B have greater impact parameter d_0 , a cut using the resolution achieved by the HFT based on a minimal value of d_0 is possible. In this study B^+ and D^+ are embedded in HIJING central events Au+Au collisions at 200 GeV. The spectra of non-photonics electrons spectra after STAR data reconstruction is measured (fig. 11). As it is seen on fig. 13 (left), there is a clear region for $4 < p_T < 5$ GeV/c where the electrons from B decays dominate ; their spectra and comparison to electrons from D are represented on fig. 13 (right).

Displaced vertices to measure contribution of electrons from indirect ($B \rightarrow J/\Psi \rightarrow e^+e^-$) and direct $J/\Psi (J/\Psi \rightarrow e^+e^-)$. This method uses a cut on the pseudo- τ defined as :

$$\tau = \vec{L} \cdot \frac{p_T^\Psi}{|p_T^\Psi|} \cdot \frac{M_\Psi}{p_\Psi}$$

Pythia J/Ψ 's are embedded in central Au+Au collisions from HIJING.

Fig 13 : (left) Impact parameter distributions of electrons from B and decays; (right) electrons yield for 200 $\mu\text{m} < d_0 < 600 \mu\text{m}$ and $p_T > 4$ GeV/c.

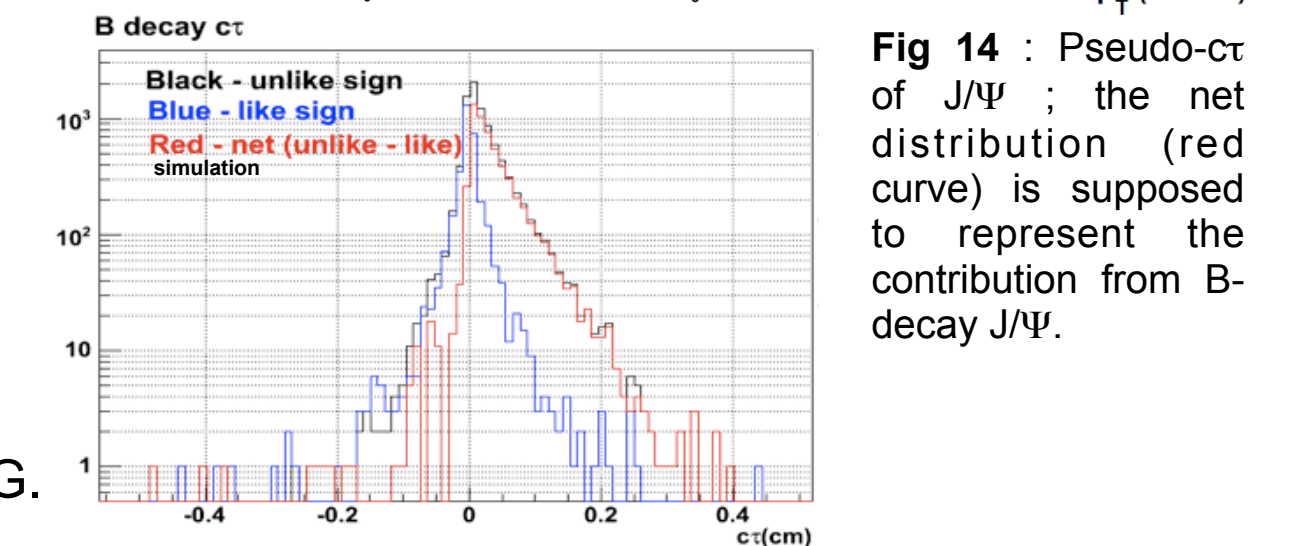
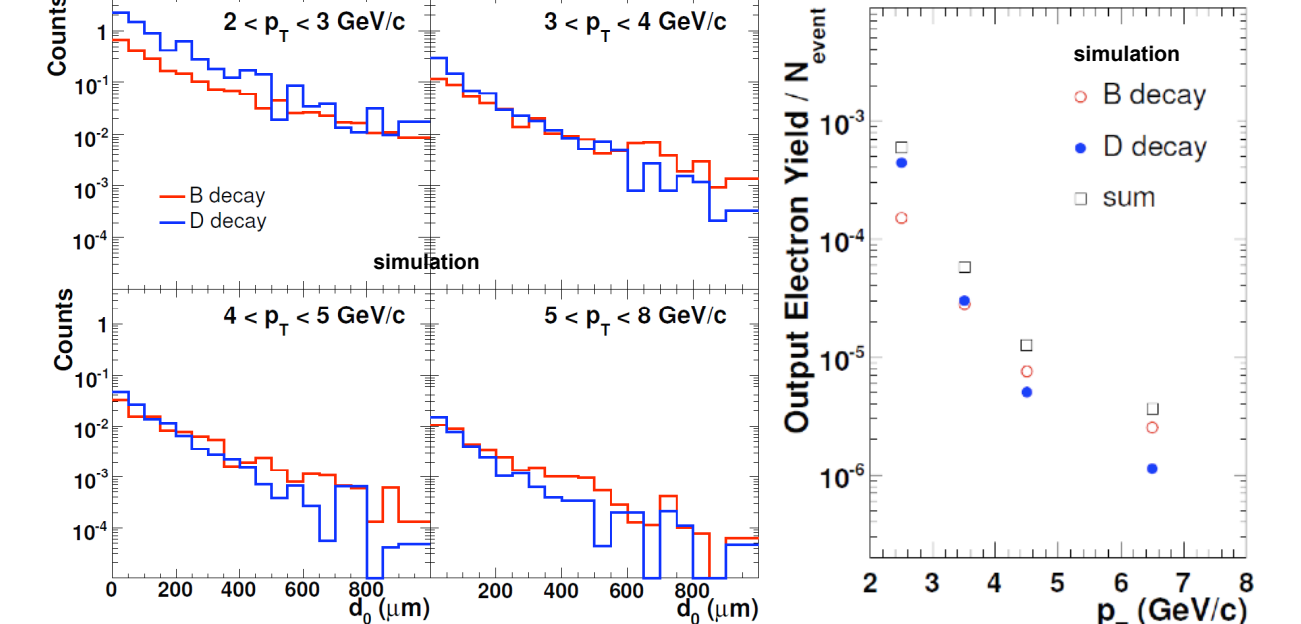


Figure 14 : Pseudo- τ of J/Ψ ; the net distribution (red curve) is supposed to represent the contribution from B-decay J/Ψ .

A realistic simulator

Calculate the number of electrons generated from charged tracks through the silicon sensor using a Bichsel distribution.

Build the geometry of the detector : 1 chip made of 640 30 $\mu\text{m} \times 50 \mu\text{m} \times 30 \mu\text{m}$ pixels composed by different layers (readout electronics, substrate and active layers).

Simulate the transportation of electrons :

- Diffusion, recombination and reflection at the interfaces between layers.
- Recalculate the number of electrons collected.

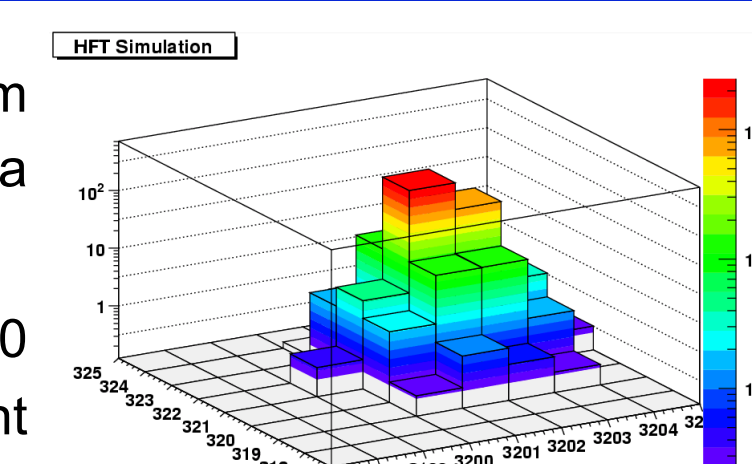


Figure 15 : (left) Reconstructed cluster profile of electrons deposited from a single track with incident angle = 45° .

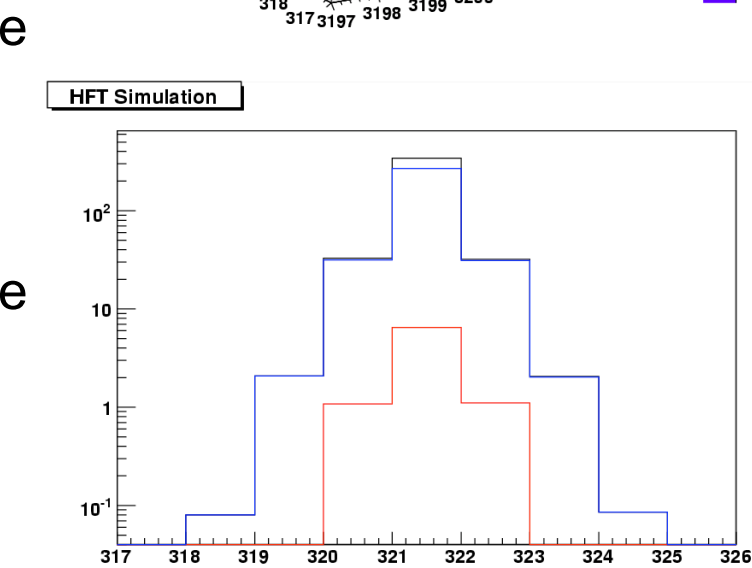


Figure 16 : (left) Distribution of the number of electrons collected by fired pixel and its neighbors and the number of electrons collected by the epitaxial layer and substrate layers. The contribution from the epitaxial layer is 81.7% and from the substrate layer : 2.1%.

Summary

The HFT will be able to reconstruct direct charm and bottom hadrons.

Pixel detector using low-mass CMOS sensors to minimize Multiple Coulomb Scattering.

Confirmation of the performances (pointing resolution, tracking efficiency) with Monte-Carlo Simulations of Au+Au collisions at 200 GeV including STAR detector response simulators.

Improvement of measurement B meson.

- Z. Lin and M.Gyulassy, phys. Rev. C77 (1996)1222
- G. Wang, J. Phys. G : Nucl. Part. Phys. 35 (2008) 104107
- E. Anderssen et al., A Heavy Flavor Tracker for STAR (http://mc.lbl.gov/hft/docs/hft_final_submission_version.pdf)
- B. Abelev et al., Phys. Rev. Lett 98 192301 (2007)
- J. Kapitan, STAR inner tracking upgrade - A performance study, proceeding of HotQuarks 2008

